Springer

KSME

Journal of Mechanical Science and Technology 31 (5) (2017) 2423~2431
www.springerlink.com/content/1738-494x(Print)/1976-3824(Online)
DOI 10.1007/s12206-017-0440-6

Topology optimization based on spline-based meshfree method using topological derivatives †

Junyoung Hur[1], Pilseong Kang[2] and Sung-Kie Youn[1,*]

[1]*Department of Mechanical Engineering, KAIST, 291 Daehak-ro, Yuseong-gu, Daejeon 305-701, Korea*
[2]*Center for Space Optics, Korea Research Institute of Standards and Science, 267 Gajeong-ro, Yuseong-gu, Daejeon 34113, Korea*

(Manuscript Received November 8, 2016; Revised December 29, 2016; Accepted January 5, 2017)

Abstract

Spline-based meshfree method (SBMFM) is originated from the Isogeometric analysis (IGA) which integrates design and analysis through Non-uniform rational B-spline (NURBS) basis functions. SBMFM utilizes trimming technique of CAD system by representing the domain using NURBS curves. In this work, an explicit boundary topology optimization using SBMFM is presented with an effective boundary update scheme. There have been similar works in this subject. However unlike the previous works where semi-analytic method for calculating design sensitivities is employed, the design update is done by using topological derivatives. In this research, the topological derivative is used to derive the sensitivity of boundary curves and for the creation of new holes. Based on the values of topological derivatives, the shape of boundary curves is updated. Also, the topological change is achieved by insertion and removal of the inner holes. The presented approach is validated through several compliance minimization problems.

Keywords: Isogeometric analysis; Non-uniform rational B-spline; Spline-based meshfree method; Topological derivative; Topology optimization

1. Introduction

From the pioneering work of Bendsøe and Kikuchi [1] topology optimization becomes an innovative design technique in many engineering fields. One of the advantages of topology optimization is that creation of holes (new topology) leads to flexible design changes which were rather limited in shape and size optimizations. The most popular approach in topology optimization is the density based method. It imposes density values between 0 and 1 to each cell (finite element) and intermediate density values are prohibited by penalization [2]. One of the other approaches in topology optimization is level-set based method [3, 4] by using the implicit the level-set function.

The above approaches on topology optimization have implicit boundary representation between solid and void regions. Therefore, additional post-processing efforts for converting the optimization result into a CAD design is required. To remedy this problem, the topology optimizations with explicit boundary have been proposed through an integration of shape optimization and hole creation process [5, 6]. Furthermore, Moving morphable component (MMC) method has been proposed by controlling location, orientation and shape of structural members [7].

As an alternative of design optimization based on conventional finite element method, Isogeometric analysis (IGA) [8] were applied in structural optimization by integrating design and analysis through spline basis functions. Shape optimization methods were proposed [9, 10], and they are extended geometrically nonlinear structures [11]. Furthermore, topology optimization were proposed [12] by using trimming technique in CAD system [13, 14]. One of the advantages of the topology optimization with trimming technique is that the explicit boundary can be represented effectively with spline surfaces and curves. Therefore, design dependent load problems can be easily treated and additional post processing of an optimal design to obtain a CAD file is not required.

However, the topology optimization with trimming technique has a drawback in obtaining shape sensitivity of boundary trimming curves. Since the mathematical relation between a spline surface and trimming curves does not exist, the shape sensitivity analysis on a trimming curve requires semi-analytic approach to obtain the relationship between trimming curves and spline surface. It requires a cumbersome process in the sensitivity analysis and additional computational efforts. In this research, an alternative method is proposed for updating the shape of trimming curves by using the topological derivative. Topological derivative is related to the creation of small hole within the design domain and it is applied in several researches on the topology optimization. Céa et al. [15] removed

*Corresponding author. Tel.: +82 423503034, Fax.: +82 423503210
E-mail address: skyoun@kaist.ac.kr
† Recommended by Associate Editor Gil Ho Yoon

finite elements based on the topological derivatives. Lee et al. [16] utilized topological derivative to create new holes during the shape optimization process. Furthermore, topological derivative is incorporated into the level-set based method [17] and the density based method [18].

The contents of this paper are organized as follows. In Sec. 2, Preliminaries on B-splines, Non-uniform rational B-spline (NURBS) and IGA will be briefly reviewed. The explanations on trimming technique and Spline-based meshfree method (SBMFM) will be given with the detection and integration schemes of trimmed elements. In Sec. 3, the proposed optimization approach will be given. In Sec. 4, numerical examples on topology optimization will be shown, then conclusions and future works will be presented in the last section.

2. Preliminaries

2.1 B-splines and Isogemetric analysis

B-spline basis functions are defined from a knot vector, which defines the segment of a curve or surface:

$$\mathbf{U} = \left\{u_0, u_1, ..., u_{n+p-1}, u_{n+p}\right\}, \tag{1}$$

where p is the degree of basis functions and n is the number of control points. The whole interval $\left[u_0, u_{n+p}\right]$ is called a *patch*, and the sub-interval $\left[u_i, u_{i+1}\right)$ is called *i-th knot span*, which defines the segment or an element in the parametric space. The *p-th* order B-spline basis functions are defined in recursive way as follows:

$$N_{i,p}(u) = \frac{u-u_i}{u_{i+p}-u_i} N_{i,p-1}(u) + \frac{u_{i+p+1}-u}{u_{i+p+1}-u_{i+1}} N_{i+1,p-1}(u) \quad , \tag{2}$$

with i = 1,…,n+p+1. Then, the B-spline curve is expressed as a linear combination of the basis functions and the control points:

$$\mathbf{C}(u) = \sum_{i=1}^{n} N_{i,p}(u)\mathbf{P}_i \ , \tag{3}$$

where control points $\mathbf{P}_i$ define the shape of curve. Similarly, a B-spline surface is defined by the bi-variate tensor products form of two parameters as shown in Eq. (4).

$$\mathbf{S}(u,v) = \sum_{i=1}^{n}\sum_{j=1}^{m} N_{i,p}(u) N_{j,q}(v)\mathbf{P}_{ij} \ . \tag{4}$$

NURBS is defined by imposing weights on control points and constructing rational form of basis functions. NURBS is able to express circles or conics exactly. Mathematical forms of a NURBS curve and surface are shown in Eqs. (5) and (6).

$$C(u) = \sum_{i=1}^{n} \frac{w_i N_{i,p}(u)}{\sum_{j=1}^{n} w_j N_{j,p}(u)} \mathbf{P}_i = \sum_{i=1}^{n} R_{i,p}(u)\mathbf{P}_i \tag{5}$$

$$\mathbf{S}(u,v) = \sum_{i=1}^{n}\sum_{j=1}^{m} \frac{w_{ij} N_{i,p}(u) N_{j,q}(v)}{\sum_{k=1}^{n}\sum_{l=1}^{m} w_{kl} N_{k,p}(u) N_{l,q}(v)} \mathbf{P}_{ij} \ . \tag{6}$$

IGA utilizes NURBS basis function in geometric representation and finite element analysis. Instead of using nodes and elements in finite element model, IGA uses the geometric information (knot vectors, weights and control points) from the standard CAD formats. Number of degree of freedom is easily controlled by the knot-insertion algorithm [19] which is widely used in CAD. One of the main advantages of IGA is that the exact geometry is represented by using spline basis. Moreover, its accuracy [20] and higher robustness under mesh distortion [21] have been reported.

2.2 Trimmed surface analysis and spline-based meshfree method

Rather than tensor-products form of NURBS surface used in IGA, CAD system uses trimming technique to represent complex geometry. Fig. 1 demonstrates an example of modelling process using spline basis. If the desired geometry is a simple trapezoidal surface with one inner hole, additional remodeling is required in the IGA. This remodeling includes dividing the surface into several tensor-product NURBS patches. On the other hand, trimming technique does not require any dividing process since trimming curves are utilized to cut off the unnecessary regions.

To utilize the trimming technique into IGA, Trimmed surface analysis (TSA) [13] has been proposed. In this following, main features of TSA will be briefly introduced. In TSA, Initial graphic exchange specification (IGES) format is used to export trimming information from CAD and the followings demonstrate contents of IGES file.

- Untrimmed surface information: It contains knot vectors, the degree and control point information of the NURBS surface before trimming operation is applied.
- Trimming curve information in the parametric and physical spaces: It contains knot vectors, the degree and control point information of trimming curves which are represented in the parametric and physical spaces. Note that the trimming curves in the parametric and physical spaces are defined independently.
- Direction of a trimming curve is counter-clockwise. Void region is the right side of the increasing direction of knot values while the material region is the left side. Based on the directional property of a trimming curve, a searching scheme is applied whether a certain point is in the material region or not.

After the searching scheme is applied, the elements in the analysis domain are categorized and classified into three groups depending on the number of vertex located in void region. Fig. 2 illustrates three types of trimmed element where type A has one void vertex, type B and C have two and three

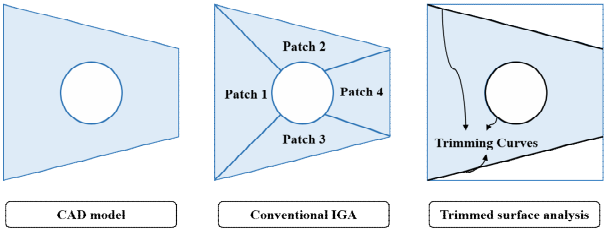

Fig. 1. An example of modelling process in IGA and TSA.

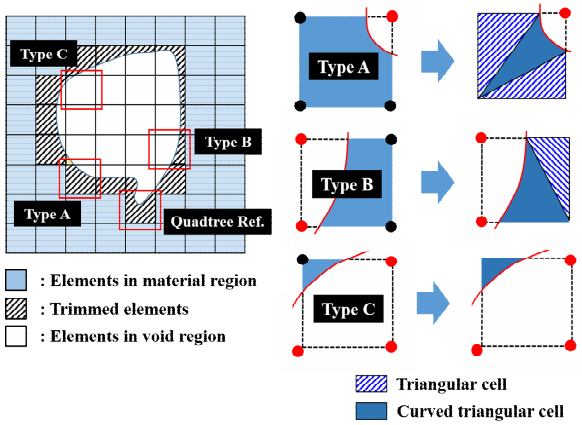

Fig. 2. Classification and decomposition of trimmed elements.

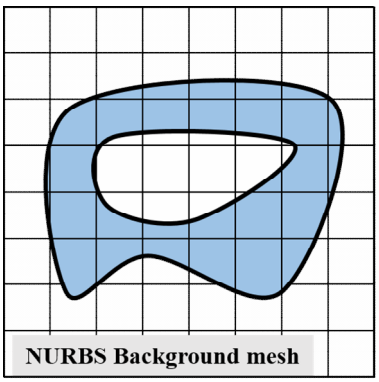

Fig. 3. Schematic representation of SBMFM.

void vertices. These types are decomposed into normal triangular cells and triangular cells with one NURBS curve. If an element cannot be classified into one of these three types, further quadtree refinement is applied. For the numerical integration of the normal triangular and the non-trimmed (rectangular) elements, the conventional IGA integration scheme can be employed. On the other hand, the triangular cells with NURBS curve uses the NURBS-enhanced integration scheme [22].

Based on TSA, Kim and Youn [23] proposed SBMFM. The conceptual sketch of SBMFM is illustrated in Fig. 3. The concept of SBMFM is to represent the analysis domain with trimming curves only and the NURBS surface acts as a background mesh. SBMFM provides the flexibility in geometry representation of complex topology with explicit boundary.

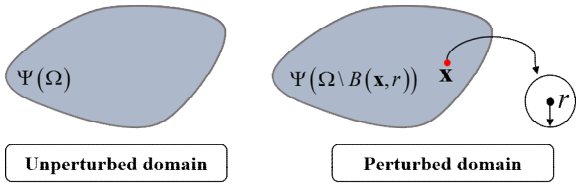

Fig. 4. Definition of topological derivative with infinitesimal perturbation.

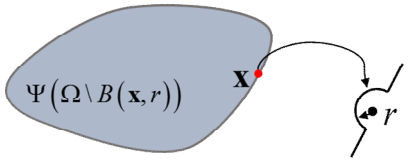

Fig. 5. Perturbation of infinitesimal domain at the boundary.

Also, robustness in nonlinear analysis is guaranteed since it does not suffer mesh distortion problem.

3. Topology optimization using SBMFM

3.1 Topological derivative based approach

As shown in Fig. 4, let $B(\mathbf{x},r)$ be a small circular hole of radius r centered at $\mathbf{x} \in \Omega$. The topological derivative of a response function Ψ with respect to the small perturbation $B(\mathbf{x},r)$ is defined as follows:

$$\Psi' = \lim_{r \to 0} \frac{\Psi(\Omega \setminus B(\mathbf{x},r)) - \Psi(\Omega)}{f(r)}, \tag{7}$$

where $f(r)$ is the positive function having the same order with spatial dimension (2 or 3). When a circular domain is perturbed in the two-dimensional space with its radius r, it is shown that

$$f(r) = \pi r^2. \tag{8}$$

For the case of compliance and 2-D elasticity problems, it is shown that the topological derivative is related to the strain energy density [24, 25] which is expressed as follows:

$$\Psi' = \frac{2}{1+\nu}\boldsymbol{\sigma}^{\mathrm{T}}\boldsymbol{\varepsilon} + \frac{3\nu - 1}{2(1-\nu^2)}\mathrm{tr}(\boldsymbol{\sigma})\mathrm{tr}(\boldsymbol{\varepsilon}), \tag{9}$$

where ν is the Poisson's ratio, $\boldsymbol{\sigma}$ and $\boldsymbol{\varepsilon}$ are stress and strain vector.

From the definition of the topological derivative described in Eq. (7), topological asymptotic expansion [26] is defined as:

$$\Psi(\Omega \setminus B(\mathbf{x},r)) = \Psi(\Omega) + f(r)\Psi'(\mathbf{x}) + o(f(r)) \tag{10}$$

where $o(f(r))$ is the higher order term of r.

Consider the perturbation is occurred on the boundary as

shown in Fig. 5, then the function $f(r)$ is defined as:

$$f(r)=\frac{1}{2}\pi r^2, \tag{11}$$

which is the same as the area of the half-circle with radius r. In this case, the topological derivative can be considered as the singular limit of the shape derivative.

From the asymptotic expansion written in Eq. (10), take the derivative this equation with respect to r and neglect $o(f(r))$, then Eq. (10) becomes as follows:

$$\frac{d}{dr}\Psi(\Omega\setminus B(\mathbf{x},r))=\frac{df(r)}{dr}\Psi'(\mathbf{x}). \tag{12}$$

Eq. (12) implies that the sensitivity of the response function with respect to the perturbation at the boundary with radius r. In this work, Eq. (12) is applied to obtain the sensitivity of trimming curves.

3.2 Boundary evolution scheme

Based on the topological asymptotic expansion described in the previous section, design update is performed from the topological derivatives which are calculated at trimming curves. Fig. 6 illustrates boundary update scheme. Let $\mathbf{P}_i^k$ be i-th control point (blue squares on Fig. 6) at k-th iteration. Then sampling points (red circles on Fig. 6) are located on this trimming curve which are denotes as $\mathbf{x}_i^k$'s and they are designated as design variables. The sensitivities of sampling points are obtained based on Eq. (12), and the optimizer returns the radius r_i^k's of each sampling point.

The location of i-th sampling point at next iteration $\mathbf{x}_i^{k+1}$ is updated based on the r_i^k and its normal vector $\mathbf{n}_i^k$. Using the updated positions of the sampling points, the shape of the trimming curve is evolved by updating the location of control points $\mathbf{P}_i^{k+1}$'s using the least-square fitting algorithm [19].

3.3 Verification of shape evolution

In this subsection, the relationship between topological derivative and evolution of trimming curve is validated. Fig. 7 illustrates problem definition of the validation model. A short cantilever beam problem with aspect ratio of 8:5 is considered with downward point load. Young's modulus and Poisson's ratio are equal to be 210 GPa and 0.3, respectably. As shown in the Fig. 8, finite difference method is applied by perturbing certain sampling points on trimming curves and evolve trimming curve by fitting method. Based on Eq. (7), following criteria is computed:

$$\frac{\Psi(\Omega\setminus B(\mathbf{x},r))-\Psi(\Omega)}{meas(\Omega\setminus B(\mathbf{x},r))-meas(\Omega)}, \tag{13}$$

where $meas$ indicates the area of the domain. Eq. (13) is

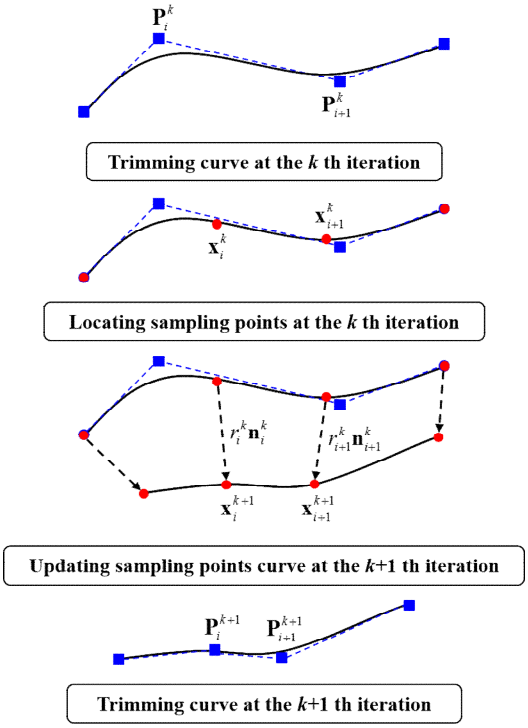

Fig. 6. Illustration of boundary evolution scheme.

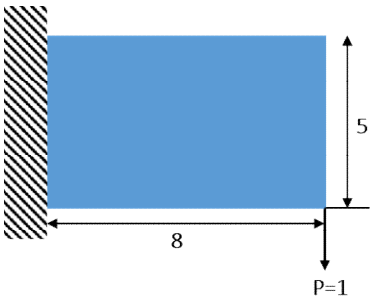

Fig. 7. The model for validation of topological derivative.

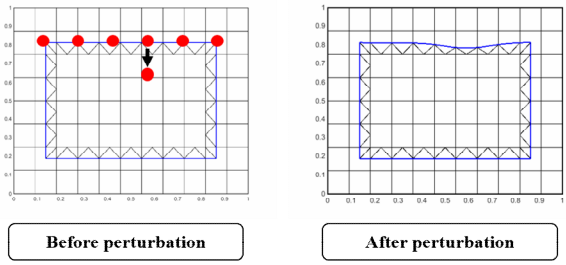

Fig. 8. Perturbation scheme of validation model.

compared with the analytic value of topological derivative of compliance. The validation is performed with following variables.

- Discretization level of background mesh: 11by 8, 20 by 15, 33 by 24 background meshes with quadratic B-spline basis function.
- Discretization level of trimming curve: 4, 10, 18 control

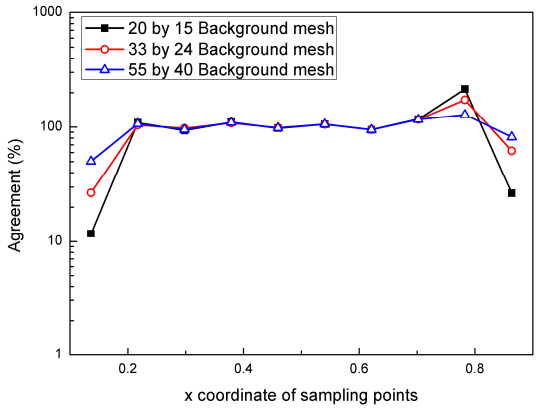

Fig. 9. Validation result w.r.t discretization level of background mesh.

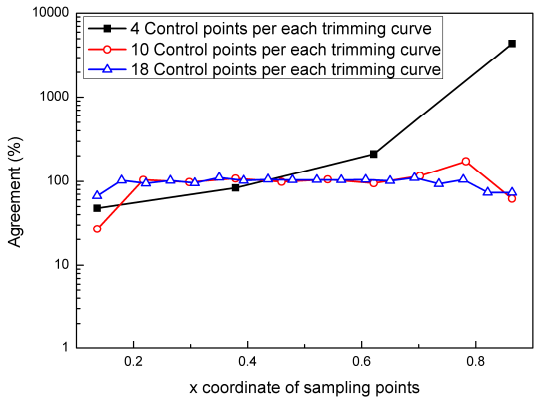

Fig. 10. Validation result w.r.t discretization level of trimming curves.

points per each trimming curve. The basis function of trimming curve is quadratic.

- Perturbation of sampling points: 0.01, 0.001 and 0.0001 in the parametric space.

Fig. 9 illustrates the influence of background mesh with 10 control points per each trimming curve and perturbation of 0.001. The x and y coordinates of this figure indicate location of sampling points at upper side of trimming curve and relative agreement between analytic topological derivative and Eq. (13). There exist higher disagreement at the corner of curves. But they are decreasing with increasing level of discretization. Fig. 10 illustrates the influence of trimming curve discretization with 33 by 24 background mesh and perturbation of 0.001. It is shown that significant errors are appeared when trimming curve has insufficient discretization since topological derivative based approach in this work is related to the creation of half circle on boundary. Fig. 11 shows the influence of perturbation with 33 by 24 background mesh and 10 control points per each curve. It is shown that excessive level of perturbation leads to the significant error in curve evolution.

Through validation process, it is shown that level of trimming curve discretization and perturbation of sampling point are important factors in the accuracy of proposed method. Based on these results, degree of freedom and move limit of

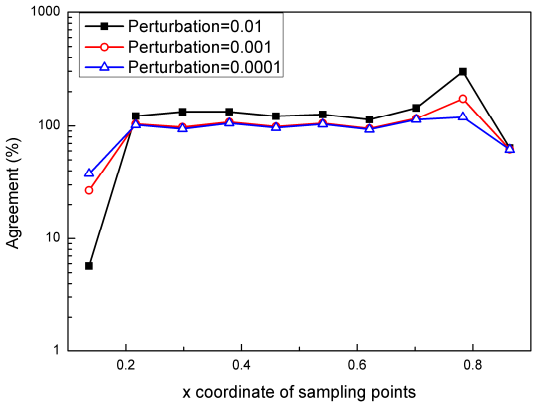

Fig. 11. Validation result w.r.t perturbation level of sampling points.

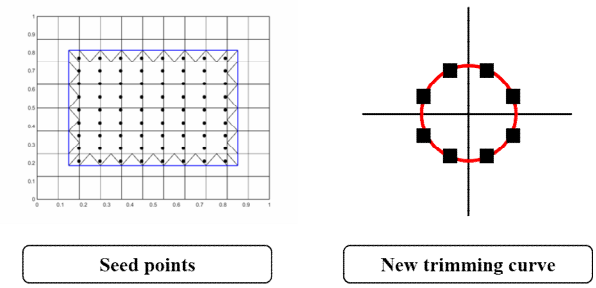

Fig. 12. Creation of new trimming curve.

trimming curves are determined to maintain a certain level of accuracy.

3.4 Creation of new hole

To determine the creation of a new holes (topological changes), seed points are created inside of the domain as shown in Fig. 12. Then obtained topological derivatives at the seed points (black circles on Fig. 12) are compared with the topological derivatives at the boundary sampling points. In this work, the minimum topological derivative of the seed points $\min(\Psi')_{seed}$ and the sampling points $\min(\Psi')_{samp}$ are compared. If the following relation is satisfied,

$$\min(\Psi')_{seed} < \min(\Psi')_{samp}, \tag{14}$$

a new NURBS trimming curve is inserted at the seed point having minimum topological derivative.

3.5 Optimization formulation and procedures

In this work, compliance minimization problem with volume constraint is concerned. The mathematical form of the optimization problem is stated as following:

$$\begin{aligned} &\underset{\mathbf{r}}{\text{minimize}} \quad \Psi = \int_{\Omega} \mathbf{b}^T \mathbf{u} d\Omega + \int_{\Gamma_t} \mathbf{t}^T \mathbf{u} ds \\ &\text{subject to} \quad G = \int_{\Omega} d\Omega - V_{req} \le 0 \end{aligned}, \tag{15}$$

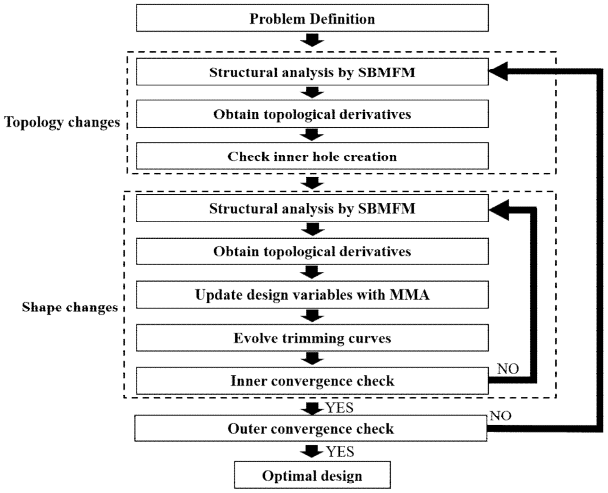

Fig. 13. Optimization procedures.

where $\mathbf{r}$ denotes the radii of sampling points, $\mathbf{u}$ is the displacement field, $\mathbf{b}$ is the body force, $\mathbf{t}$ is the traction at the region Γ_t and V_{req} represents upper limit of the volume constraint.

The overall process of this work is summarized in Fig. 13. Before trimming curves are evolved, topological changes are judged by comparing the topological derivatives of the sampling points on the trimming curves and of the interior seed points. Then shapes of the trimming curves are optimized using the Method of moving asymptotes [27] within the inner loop. After inner loop is converged, the convergence is also checked whether the outer convergence is satisfied or not. In this work, the convergence criterion is based on the changes in the objective function at the current iteration (Ψ^k) and the previous one (Ψ^{k-1}) based on the following criterion:

$$\left|\frac{\Psi^k - \Psi^{k-1}}{\Psi^{k-1}}\right| < \varepsilon, \tag{16}$$

where ε indicates the measure of convergence. The value of ε at the inner and outer loops are 10^{-2} and 10^{-4}, respectively.

4. Numerical examples

In this section, several compliance minimization problems are presented to validate the effectiveness of the proposed approach. Plane stress with linear elastic behavior is assumed. Young's modulus and Poisson's ratio are equal to be 210 GPa and 0.3, respectably.

4.1 Short cantilever beam with fixed design space

Fig. 14 illustrates the problem definition of the short cantilever beam problem with a downward point load. The upper limit of the volume fraction is 60 % of the initial value. The right side of Fig 14 shows the initial domain in the parametric space with the background mesh and 4 trimming curves. The background mesh is discretized with 20 by 15 elements by using quadratic NURBS basis functions. Trimming curves consist with quadratic B-spline curves with 10 control points and 20 sampling points for each curve.

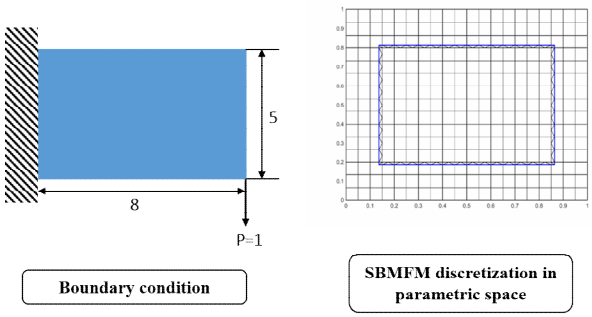

Fig. 14. Problem definition of short cantilever beam problem with fixed design space.

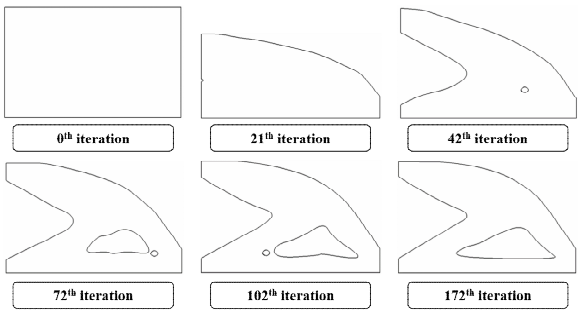

Fig. 15. History of design change in physical space of short cantilever beam problem with fixed design space.

The optimization is converged at 172th iteration. Fig. 15 illustrates the history of design change in physical spaces. As shown in this figure, boundary evolution of the existing trimming curves and creation of new curves at certain steps can be found. Furthermore, if two adjacent curves become too close to each other, these curves are merged into a single curve to prevent the interference between the trimming curves [12, 24] as shown in Fig. 16. Fig. 17 illustrates the convergence histories of the objective function (compliance) and the constraint (volume) which are normalized with their initial values.

4.2 Short cantilever beam with extendable design space

In the second case, the extendable design space problem is considered. Trimming curves are able to be extended in the y direction without any restriction. Fig. 18 illustrates the design changes in the physical spaces. At a certain stage, if a trimming curve reaches to the limit of the parametric space, the background mesh is adaptively extended which is proposed in the geometric nonlinear analysis with SBMFM [23] As shown in Fig. 19, the background NURBS surface in the physical space is extended with additional control points. After that, trimming curves at the parametric space are relocated using the point inversion and fitting algorithms [23] since the para-

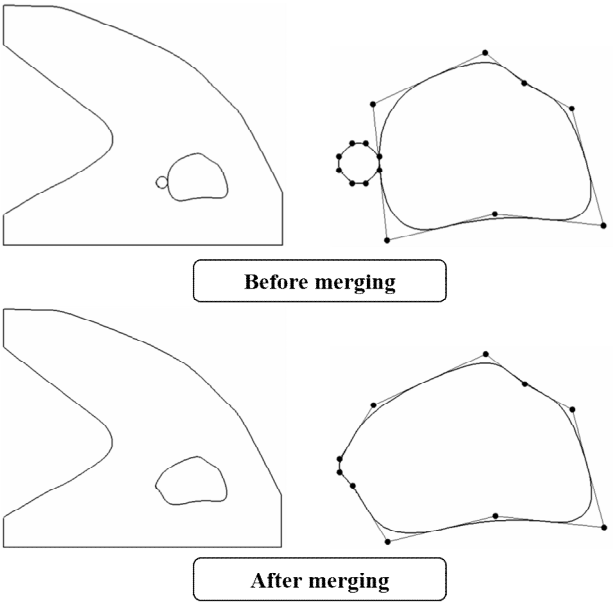

Fig. 16. Merging of trimming curves during the optimization process.

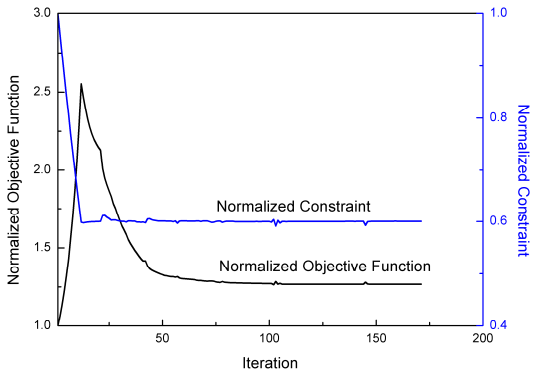

Fig. 17. Convergence histories of short cantilever beam problem with fixed design space.

metric space are always defined in the $[0,1]\times[0,1]$. Fig. 20 illustrates the convergence histories of the problem. Due to the flexibility in the design space, the normalized objective function value at the converged design (0.876) is smaller than the fixed design space case (1.28) with the same volume fraction.

4.3 Bridge beam problem

Fig. 21 illustrates the problem definition of a bridge beam problem with aspect ratio of 2:1. Due to its symmetry, a half of the domain is considered as shown in the right side of Fig. 21. In this problem, 22 by 22 elements are involved with quadratic basis functions and 4 trimming curves are used with 10 control points and 20 sampling points for each curve. The volume constraint of this problem is set to be 30 % of the initial value. Fig 22 shows the design change in the physical spaces. Fig. 23 illustrates the convergence histories of the compliance and the volume. It is shown that optimal design is converged to the truss structure to maintain the downward loading.

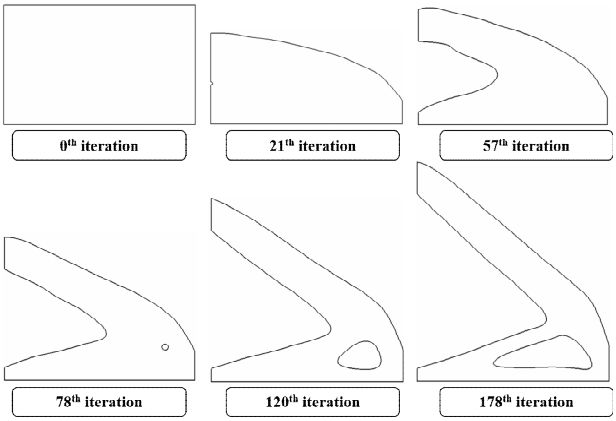

Fig. 18. History of design change in physical space of short cantilever beam problem with extendable design space.

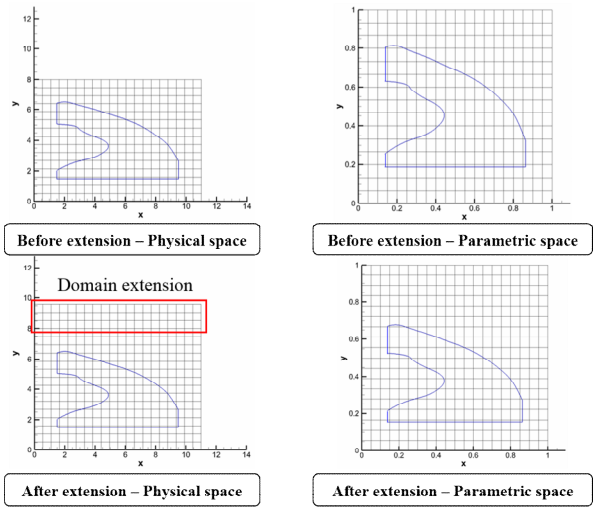

Fig. 19. An example of domain extension at 57th iteration.

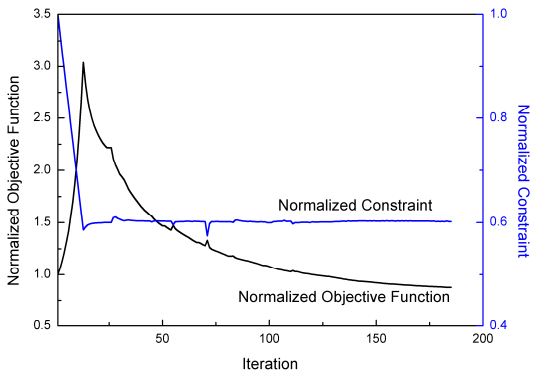

Fig. 20. Convergence histories of short cantilever beam problem with extendable design space.

5. Conclusions

In this research, the topology optimization with explicit

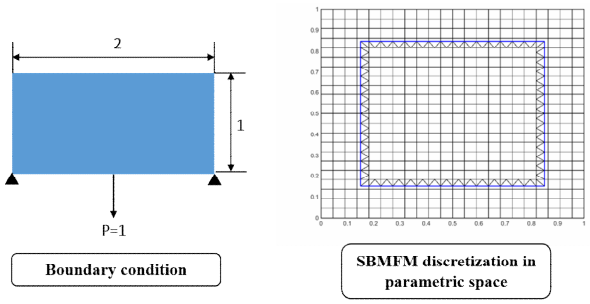

Fig. 21. Problem definition of a bridge beam problem.

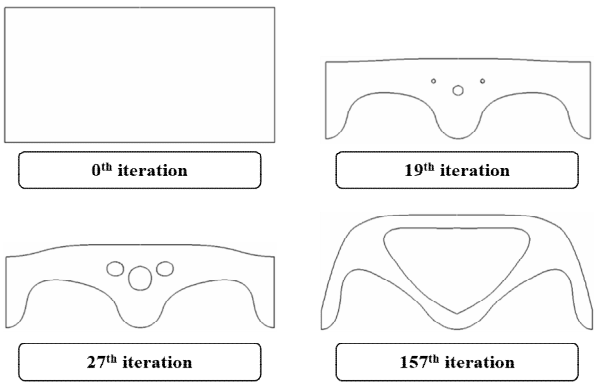

Fig. 22. History of design change in parametric space of a bridge beam problem with full model.

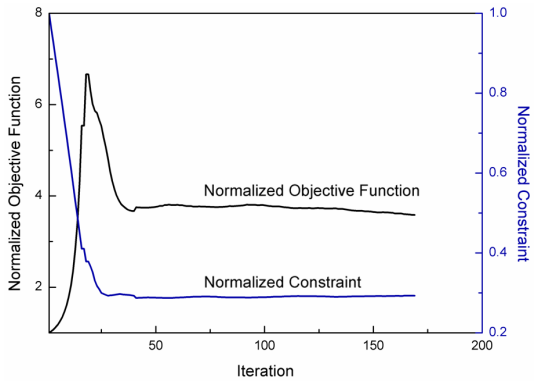

Fig. 23. Convergence histories of a bridge beam problem.

boundary representation is incorporated into the SBMFM framework. Topological derivative is applied to describe the sensitivity of trimming curves, then these curves are updated by using the curve fitting algorithm. The relationship between topological derivatives and update of trimming curve is verified numerically. Topological change is achieved by inserting new trimming curve which is determined by comparing the topological derivatives at the boundaries and the inside evaluation points of the design domain. Proposed approach is validated through several numerical examples. It is shown that the inserting and merging of trimming curves describe topological changes appropriately while explicit and smooth boundary representation of SBMFM is maintained. Furthermore, the extendable design space problem is easily treated by adaptive extension of the NURBS background mesh.

Compared with the previous work [12], one of the advantages of using SBMFM is that relocation of the non-design control points during the optimization is neglected. Proposed method alternates sensitivity analysis and update of trimming curves. By using analytic sensitivity formulation using topological derivatives, additional computational costs and cumbersome process of previous work are reduced. Furthermore, proposed method provides possibilities on extending our work to the 3-dimensional applications.

Beyond the compliance minimization problem, this study will be applied to a variety of applications such as material design and compliant design problems. Also, this work can be applied to the design dependent load problem. By using SBMFM, it will have great advantage in treating loaded boundaries.

Acknowledgment

This paper was supported by BK21 Plus Program.

References

[1] M. P. Bendsøe and N. Kikuchi, Generating optimal topologies in structural design using a homogenization method, *Computer Methods in Applied Mechanics and Engineering*, 38 (6) (1988) 535-543.

[2] M. P. Bendsøe, Optimal shape design as a material distribution problem, *Structural Optimization*, 1 (4) (1989) 193-202.

[3] T. Belytschko, S. P. Xiao and C. Parimi, Topology optimization with implicit functions and regularization, *International Journal for Numerical Methods in Engineering*, 57 (8) (2003) 1177-1196.

[4] M. Yulin and W. Xiaoming, A level set method for structural topology optimization and its applications, *Advances in Engineering Software*, 35 (7) (2004) 415-441.

[5] H. A. Eschenauer, V. V. Kobelev and A. Schumacher, Bubble method for topology and shape optimization of structures, *Structural Optimization*, 8 (1) (1994) 42-51.

[6] A. N. Christiansen, M. Nobel-Jørgensen, N. Aage, O. Sigmund and J. A. Bærentzen, Topology optimization using an explicit interface representation, *Structural and Multidisciplinary Optimization*, 49 (3) (2014) 387-399.

[7] X. Guo, W. Zhang and W. Zhong, Doing Topology Optimization Explicitly and Geometrically—A New Moving Morphable Components Based Framework, *Journal of Applied Mechanics,* 81 (8) (2014) 081009.

[8] T. J. R. Hughes, J. A. Cottrell and Y. Bazilevs, Isogeometric analysis: CAD, finite elements, NURBS, exact geometry and mesh refinement, *Computer Methods in Applied Mechanics and Engineering*, 194 (39-41) (2005) 4135-4195.

[9] W. A. Wall, M. A. Frenzel and C. Cyron, Isogeometric structural shape optimization, *Computer Methods in Applied*

Mechanics and Engineering, 197 (33-40) (2008) 2976-2988.
[10] S. Cho and S. H. Ha, Isogeometric shape design optimization: Exact geometry and enhanced sensitivity, *Structural and Multidisciplinary Optimization*, 38 (1) (2009) 53-79.
[11] B. Koo, S.-H. Ha, H.-S. Kim and S. Cho, Isogeometric Shape Design Optimization of Geometrically Nonlinear Structures, *Mechanics Based Design of Structures and Machines*, 41 (3) (2013) 337-358.
[12] Y.-D. Seo, H.-J. Kim and S.-K. Youn, Isogeometric topology optimization using trimmed spline surfaces, *Computer Methods in Applied Mechanics and Engineering*, 199 (49-52) (2010) 3270-3296.
[13] H.-J. Kim, Y.-D. Seo and S.-K. Youn, Isogeometric analysis for trimmed CAD surfaces, *Computer Methods in Applied Mechanics and Engineering*, 198 (37-40) (2009) 2982-2995.
[14] H.-J. Kim, Y.-D. Seo and S.-K. Youn, Isogeometric analysis with trimming technique for problems of arbitrary complex topology, *Computer Methods in Applied Mechanics and Engineering*, 199 (45-48) (2010) 2796-2812.
[15] J. Céa, S. Garreau, P. Guillaume and M. Masmoudi, The shape and topological optimizations connection, *Computer Methods in Applied Mechanics and Engineering*, 188 (4) (2000) 713-726.
[16] S. Lee, B. Kwak and I. Kim, Smooth boundary topology optimization using B-spline and hole generation, *International Journal of CAD/CAM,* 7 (1) (2007).
[17] M. Burger, B. Hackl and W. Ring, Incorporationg topological derivatives into level set methods, *Jouranl of Computational Physics*, 194 (1) (2004) 344-362.
[18] S. Amstutz, Connections between topological sensitivity analysis and material interpolation schemes in topology optimization, *Structural and Multidisciplinary Optimization*, 43 (6) (2011) 755-765.
[19] P. Les and W. Tiller, *The NURBS book*, Second Ed., Springer-Verlag, New York, USA (1997).
[20] J. A. Cottrell, T. J. R. Hughes and Y. Bazilevs, *Isogeometric Analysis: Toward Integration of CAD and FEA,* Wiley (2009).
[21] S. Lipton, J. A. Evans, Y. Bazilevs, T. Elguedj and T. J. R. Hughes, Robustness of isogeometric structural discretizations under severe mesh distortion, *Computer Methods in Applied Mechanics and Engineering*, 199 (5-8) (2010) 357-373.
[22] R. Sevilla, S. Fern´andez-M´endez and A. Huerta, NURBS-enhanced finite element method (NEFEM), *International Journal for Numerical Methods in Engineering*, 76 (1) (2008) 56-83.
[23] H.-J. Kim and S.-K. Youn, Spline based meshfree method, *International Journal for Numerical Methods in Engineering*, 92 (9) (2012) 802-834.
[24] P. Kang and S.-K. Youn, Isogeometric topology optimization of shell structures using trimmed NURBS surfaces, *Finite Elements in Analysis and Design*, 120 (1) (2016) 18-40.
[25] A. A. Novotny, R. A. Feijóo, E. Taroco and C. Padra, Topological sensitivity analysis, *Computer Methods in Applied Mechanics and Engineering*, 192 (7-8) (2003) 803-829.
[26] J. Sokolowski and A. Zochowski, On the topological derivative in shape optimization, *Inria Report* (1999).
[27] K. Svanberg, The method of moving asymptotes—a new method for structural optimization, *International Journal for Numerical Methods in Engineering*, 24 (2) (1987) 359-373.

Junyoung Hur received B.S. and M.S. degrees in Mechanical Engineering from KAIST, Korea. He is currently a Ph.D. candidate in Mechanical Engineering at KAIST, Korea. His research interest includes design optimization through spline basis functions.

Sung-Kie Youn is a Professor of Mechanical Engineering at KAIST, Korea. He received his Ph.D. in University of Texas at Austin. He joined KAIST in 1988. His research interest include computational mechanics and design optimization.